รายงานวิจัยฉบับสมบูรณ์

โครงการ การใช้แกรฟีนเป็นสารเติมแต่งนาโนชีทเพื่อปรับปรุงคุณสมบัติของพลาสติกที่ย่อยสลายได้ตามธรรมชาติ

โดย ผศ.ดร.วิศณุสรรค์ ชาติอารยะวดี

มิถุนายน 2558

สัญญาเลขที่ MRG5680066

รายงานวิจัยฉบับสมบูรณ์

โครงการ การใช้แกรฟีนเป็นสารเติมแต่งนาโนชีทเพื่อปรับปรุงคุณสมบัติของพลาสติกที่ย่อยสลายได้ตามธรรมชาติ

ผศ.ดร.วิศณุสรรค์ ชาติอารยะวดี มหาวิทยาลัยพะเยา

สนับสนุนโดยสำนักงานกองทุนสนับสนุนการวิจัย

กิตติกรรมประกาศ

งานวิจัยนี้สำเร็จลุล่วงไปด้วยดีตามวัตถุประสงค์ด้วยความร่วมมือจากหลายฝ่ายที่เกี่ยวข้อง ผู้วิจัยขอขอบคุณสำนักงานคณะกรรมการการอุดมศึกษา สำนักงานกองทุนสนับสนุนการวิจัยและมหาวิทยาลัยพะเยาที่ให้ทุนสนับสนุนการวิจัยตลอดทั้งโครงการ ขอขอบพระคุณภาควิชาเคมี คณะวิทยาศาสตร์ มหาวิทยาลัยพะเยา สำหรับสถานที่ในการทำวิจัย ขอขอบคุณ ดร.โรเบิร์ต มอลลอย ที่ช่วยให้คำปรึกษาและการชี้แนะเป็นอย่างดี

รูปแบบ Abstract (บทคัดย่อ)

Project Code : MRG5680066
รหัสโครงการ : MRG5680066

Project Title : Graphene as a Nanosheet Filler for Property Enhancement in Bioplastics
ชื่อโครงการ : การใช้แกรฟีนเป็นสารเติมแต่งนาโนชีทเพื่อปรับปรุงคุณสมบัติของพลาสติกที่ย่อยสลายได้ตามธรรมชาติ

Investigator : ผศ.ดร.วิศณุสรรค์ ชาติอารยะวดี มหาวิทยาลัยพะเยา
ชื่อนักวิจัย : Asst. Prof. Dr. Widsanusan Chartarrayawadee

E-mail Address : widsanusan@hotmail.com

Project Period : June 3th 2013 – June 2 th 2015
ระยะเวลาโครงการ : 3 เดือน มิถุนายน พ.ศ 2556 ถึง วันที่ 2 เดือน มิถุนายน พ.ศ 2558

For the purpose of development of graphene/polylactic acid (PLA) composites with improved mechanical properties, a stearic acid (SA) compatibilizer was used to enhance the compatibility of graphene oxide sheets (GO) to PLA polymer matrix. Graphene oxide was modified with stearic acid at different mass ratios of 1, 3 and 5 prior to forming composites with PLA. Characterization showed positive effects of SA attached to GO in every mass ratio and also compatibility with PLA matrix. SA can strengthen interfacial interactions of flat graphene sheets with polymer matrices resulting in polymer properties improvement. The tensile strength of PLA-GO-SA composites with mass ratio of 1 increases almost 35 percent compared to neat PLA. The results implied that GO-SA composites can be used as a nanosheet filler for property enhancement in PLA.

Keywords : Graphene, Polylactic acid, Bioplastic, Stearic acid

งานวิจัยนี้มุ่งพัฒนาสมบัติเชิงกลของคอมโพสิตแกรฟีน/กรดพอลิแลกติกโดยใช้กรดสเตียริกเป็นสารช่วยประสานเพื่อเพิ่มความเข้ากันได้ระหว่างแผ่นแกรฟีนและเนื้อพอลิเมอร์ ในงานวิจัยนี้แกรฟีนออกไซด์ถูกดัดแปลงโครงสร้างด้วยกรดสเตียริกที่ 1, 3 และ 5 อัตราส่วนโดยมวลก่อนทำการคอมโพสิทร่วมกับกรดพอลิแลกติก จากการหาลักษณะเฉพาะพบว่ากรดสเตียริกสามารถเข้าจับกับแกรฟีนออกไซด์ได้ในทุกอัตราส่วนโดยมวลและมีความเข้ากันได้กับเนื้อพอลิเมอร์ กรดสเตียริกสามารถเสริมสร้างอันตรกิริยาที่รอยต่อระหว่างแผ่นแกรฟีนและเนื้อพอลิเมอร์ได้จึงส่งผลให้พอลิเมอร์มีสมบัติที่ดีขึ้น จากผลการทดลองพบว่าคอมโพสิทของกรดพอลิแลกติก แกรฟีนและกรดสเตียริกที่อัตราส่วนโดยมวลของกรดสเตียริกเท่ากับ 1 ให้ค่าความทนต่อแรงดึงเพิ่มสูงขึ้นถึง 35 เปอร์เซ็นต์เมื่อเปรียบเทียบกับคอมโพสิตของกรดพอลิแลกติกเพียงอย่างเดียวซึ่งแสดงให้เห็นว่าคอมโพสิตของแกรฟีนและกรดสเตียริกสามารถนำไปใช้เป็นสารเติมแต่งเพื่อปรับปรุงสมบัติของกรดพอลิแลกติกได้

คำหลัก : แกรฟีน กรดพอลิแลกติก, พลาสติกที่ย่อยสลายได้ตามธรรมชาติ กรดสเตียริก

Content

Introduction

Nowadays, plastics play important roles in human daily life such as in the packaging industries, general industries and pharmaceutical and medical industries. However, a huge consumption of these conventional plastics which is produced by petrochemical industries leads to environmental destruction and pollution due to their contamination of natural resources and slow degradation. With this issue in concern, people turn their attention to an environment of using materials which can be biodegraded under environmental conditions. Bioplastics, as biodegradable plastics, have received much attention from people, due to their being environmentally friendly. Bioplastics could be derived from plant-based materials such as starch and silk fibroin or synthetic biodegradable polymer such as poly(lactic acid), poly(glycolic acid) and poly(ε-caprolactone) [1-3]. Furthermore, the degradation of bioplastics yields carbon dioxide and water as end products which are friendly to an environment. So bioplastics is one of the most innovative materials which is classified as an environmentally friendly product. However, bioplastics have some drawbacks such as limited shelf life, as they degrade very quickly, and have low mechanical strength compared to regular plastics xxx.

Graphene is defined as a single layer of two-dimensional sp^2 carbon atoms arranged in a honeycomb or hexagonal ring structure obtained from the stacking of hexagonal carbon layers called graphite. Graphene has many outstanding properties, including large surface areas up to 2630 m^2g^{-1} xxx (in theory), high Young's modulus (1100 Gpa) [4] with fracture strength up to 125 GPa [4], high charge carrier mobility (200,000 $cm^2V^{-1}s^{-1}$) [5], and good thermal conductivity (5000 $Wm^{-1}K^{-1}$) [6]. All these outstanding properties make graphene a good candidate for a filler of biodegradable polymer matrix to enhance their mechanical and thermal properties. It has been reported that graphene has a potential to be used as a nanofiller with an improvement of polymer properties. Graphene/polymer composites can significantly improve tensile strength, elastic modulus, electrical and thermal properties xxx. Compared with carbon nanotubes, graphene has a higher ratio of surface-to-volume due to the inaccessibility of the inner of carbon nanotubes surface to polymer matrices [7]. This makes graphene more favorable for improving polymer properties. There have been reports that Poly(methyl methacrylate) (PMMA) [8, 9], Poly(vinyl alcohol) (PVA) [10, 11], Polystyrene (PS) [12]

were used as polymer matrices for graphene to fabricate graphene/polymer composites. It was found that these graphene/polymer composites show superior properties of mechanical, electrical and thermal properties.

In terms of the fabrication of graphene/biodegradable polymer composite, graphene can be incorporated with biodegradable polymers such as poly(lactic acid) by: (i) blending with the polymer matrix followed by curing and/or polymerization to produce graphene/polymer composites; (ii) reducing by in-situ chemical or thermal reduction of graphene oxide (GO) during blending with polymer matrix then followed by curing and/or polymerization [13]. However, preparing graphene/poly(lactic acid) (PLA) could lead to brittleness and cracking in polymer composite matrices due to the insufficient surface wettability of graphene to PLA. In this work, we try to increase surface wetting of graphene by using stearic acid (SA) modification. Graphene sheets were functionalized with the long alkyl chain from SA to increase their lipophilicity and compatibility with PLA. Furthermore, trans-esterification of PLA composite was examined.

Experimental

Materials

PLA resin (4043D) was supplied by Nature Works Co. (USA). Natural graphite powder employed in this work was SP-1 supplied by Bay Carbon (Bay City, Michigan, USA). Di-Phosphorus pentoxide was obtained from Merck. Potassium persulfate and Potassium permanganate was supplied by Ajax. Stearic acid (SA) was purchased from Loba. Sulfuric acid, THF, Methanol and Ethanol were purchased from Labscan. Titanium (IV) butoxide was purchased from Sigma-Aldrich.

Preparation of PLA and PLA/GO composite films

PLA film was firstly prepared by dissolving PLA resin 8.91 g in THF 45 ml at 50 ^{o}C and stirring until the PLA was completely dissolved followed by co-precipitation of PLA in methanol. Precipitated PLA was then dried at 70 oC in the oven for 12 hours. The obtained PLA was chopped in a Moulinex blender in readiness for film fabrication.

PLA/GO composites film was prepared by the method mentioned above. GO (0.09 g) was sonicated in 30 ml THF for 30 mins at room temperature. GO solution was then mixed with PLA solution followed by stirring, co-precipitation and powder preparation.

In this study, PLA and PLA/GO composites films were fabricated by a hot press forming process, which consisted of heating and compressing PLA powder for a measured amount of time (for 60 mins) and optimized temperature of 180 oC.

Preparation of GO-SA nanocomposite and PLA/GO-SA composite films

GO-SA nanocomposite was prepared by mixing GO (0.09 g) in ethanol (30 ml) with SA in ethanol (mass ratios of 1, 3 and 5 of GO). The mixtures were then stirred for 24 hrs and dried for 8 hours at 70 oC. GO-SA nanocomposites with mass ratios of SA to GO 1, 3 and 5 were dispersed in THF and mixed with PLA solution followed by co-precipitation in methanol and film fabrication as previously mentioned above.

Preparation of PLA/GO-SA-Ti(OBu)4 composite films

PLA/GO-SA-Ti(OBu)4 composite films were prepared by adding Ti(OBu)4 1 wt % of GO-SA nanocomposite in the mixtures of GO-SA nanocomposite and PLA in THF. Films fabrication was prepared as per the method indicated above.

Characterizations

Tensile properties of fabricated films were examined with a tensile tester (Cometech-QC506B1). Films were cut into a specimen size of 80 mm in length, 10 mm in width and 0.4 mm in thickness. The specimens were elongated at a rate of 1 mm/min.

X-ray photoelectron spectroscopy (Kratos Axis Ultra DLD X-ray Photoelectron Spectrometer) was analyzed using Al Kα X-ray radiation.

Raman spectroscopy (Model Jobin–Yvon Horiba T64000 Raman spectrometer with LabSpec software) equipped with a microscope (50x objective) and a Nd-YAG laser with excitation wavelength of 532 nm was used to record raman spectra of composite samples.

X-ray diffractometer (Rigaku Miniflex 600 X-Ray Diffractometer using Cu Kα X-ray radiation) was used to investigate the diffraction patterns of the composite samples.

Thermal analysis was analyzed by differential scanning calorimeter (PerkinElmer-DSC7). Samples were heated from room temperature to 200 oC with heating rate of 10 oC / min and then cooled down to -20 oC.

Scanning Electron Microscopy (SEM, JEOL JSM-5910LV) was used to investigate morphology and fractured surface of composite films.

Results and Discussions

Raman spectroscopy

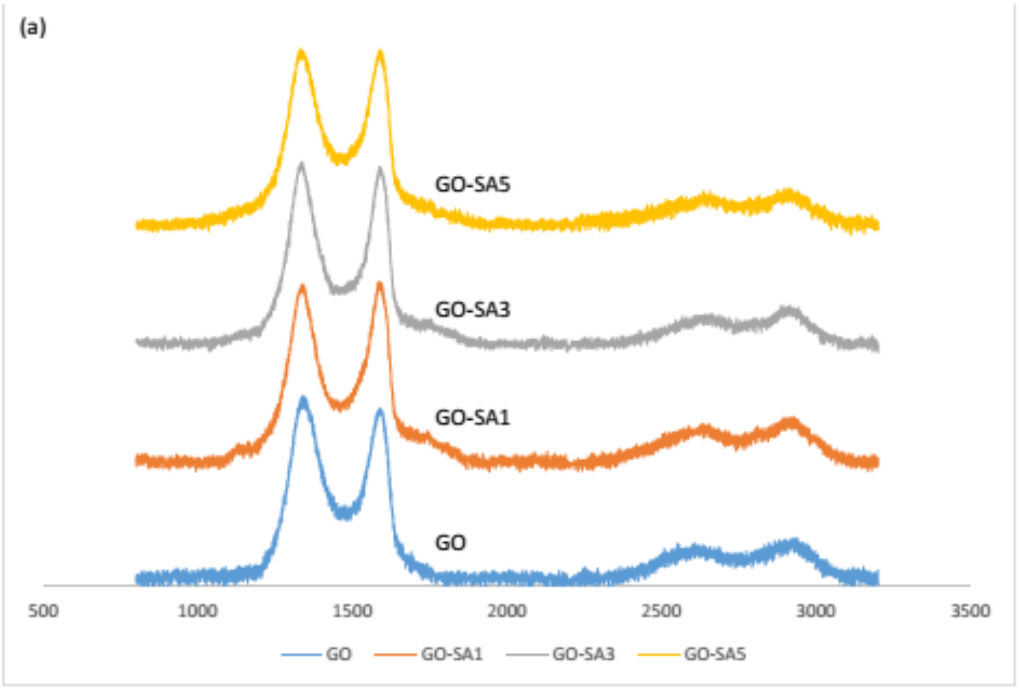

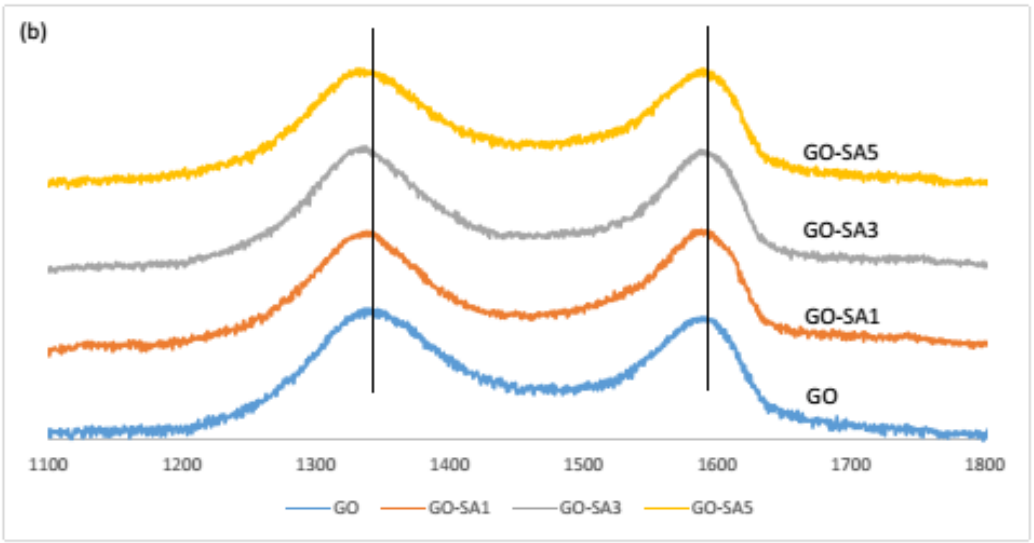

Figure 1. (a) Raman spectra of GO, GO-SA1, GO-SA3 and GO-SA5. (b) Expansion of Raman spectra of GO, GO-SA1, GO-SA3 and GO-SA5

The raman spectra (Fig. 1) of GO show D band G band and 2D band at 1352, 1577 and 2650 respectively. Generally, D and G band peaks represent the molecular response of poly-aromatic hydrocarbons in carbon materials. The D band (also known as disorder band or defect band) refers to a ring breathing mode of sp2 carbon rings G band relates to the E2g phonon of sp^2 carbon atom [14]. From Figure 1, D band of GO is dominant which indicates that there are a lot of defects in GO [15-17]. These defects come from acid oxidation in the Hummers method.

The ratio of the D to G bands intensities (I_D/I_G) in Raman spectra also informs on defect and disorder in the carbon structure [15, 16, 18]. It can be observed that the ratio of D to G band in GO is higher than 1 while the ratio of D to G band in GO-SA1, GO-SA3 and GO-SA5 are nearly or equal to one. This can be interpreted as that the addition of stearic acid to GO can decrease defects by the stearic acid coating on GO sheets, and also the ordered structure increment of graphene sheets by the agglomeration or regrouping of GO sheets encapsulated by stearic acid.

The ratio of I(G)/I(2D) band and shifting of G band is used to determine the layer thickness [14, 19, 20]. If the ratio of I(G)/I(2D) increases, the numbers of graphene layers increased. Also if G band shifts to the lower wavenumber, the layer thickness has increased [14]. From Fig. 1b, It can be observed that there is a small G peak shift to lower wavenumber in the raman spectra of GO-SA1, GO-SA3 and GO-SA. This can be an indication that SA addition to GO may induce a restacking of graphene sheets resulting in lower Raman shifts. Furthermore, the shift in D and G band peaks towards lower wavenumbers indicates the reduction of GO [16, 21]. However, in this case GO may not be reduced but the substitution of alkyl group from stearic acid to the epoxy group occurred instead by the following mechanism in Fig. 2.

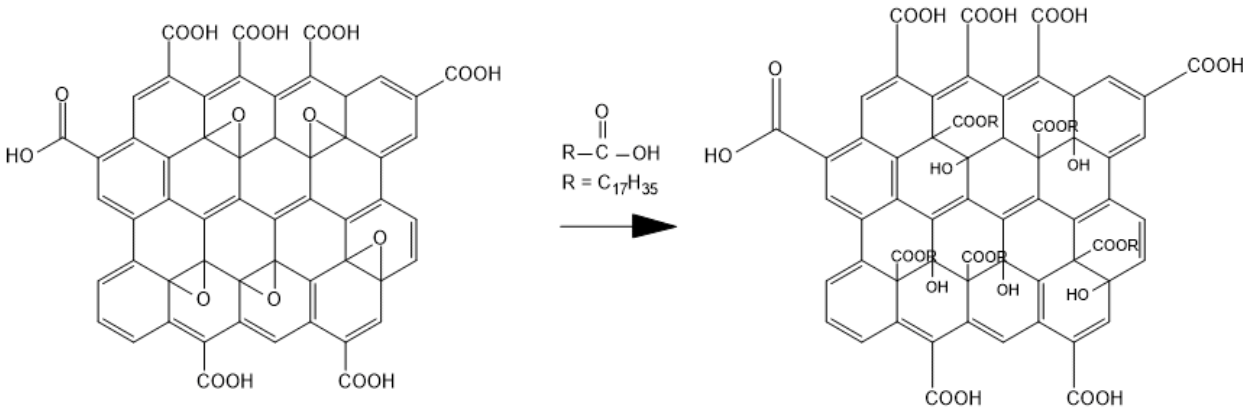

Figure 2. Schematic presentation of the substitution of alkyl group from stearic acid to the epoxy group on graphene sheet.

The reduction of the epoxy group is confirmed by XPS and will be discussed in the next section.

X-ray photoelectron spectroscopy, XPS

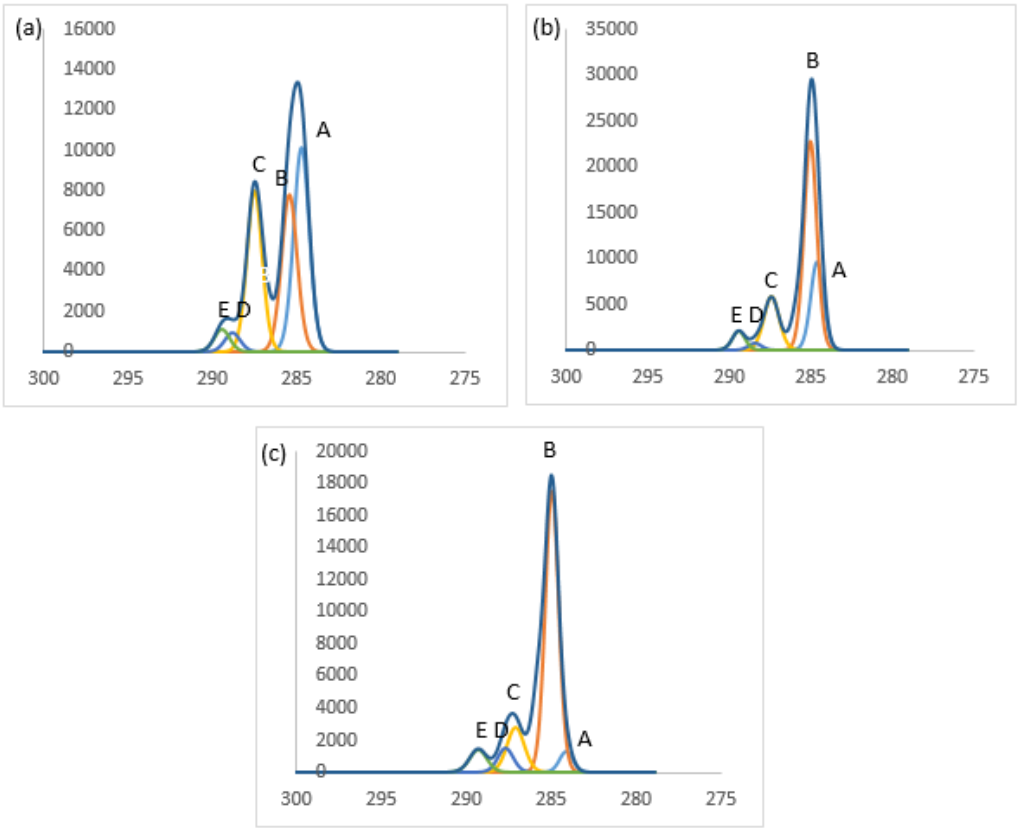

Figure 3. XPS spectra of (a) GO-SA1, (b) GO-SA3 and (c) GO-SA5

The C1S XPS spectrum of GO-SA1, GO-SA3 and GO-SA5 (Fig. 3a to c) indicates five different peaks at 284.5, 285.3, 287.2, 288.7 and 289.7 attributable to C=C (aromatic hydrocarbon), C-C/C-H (aromatic hydrocarbon), C-O (epoxy and alkoxy), C=O (carbonyl group) and O=C-O (carboxylic acid group) bonds (refer from A to E) [16]. It can be observed that the C1S spectra of C-C/C-H (Peak B) dramatically increased from GO-SA1 to GO-SA5, indicating the C-C/C-H attached on the surface of GO. These results suggest that the surface coverage of GO with stearic acid is increased with the amount of stearic acid addition. Furthermore, the decrease in peak A and peak C intensities can be confirmation of the surface coverage of GO by stearic acid because the XPS spectroscopic technique is used to analyze samples with an average depth of analysis of approximately 5 nm.

X-Ray Diffraction, XRD

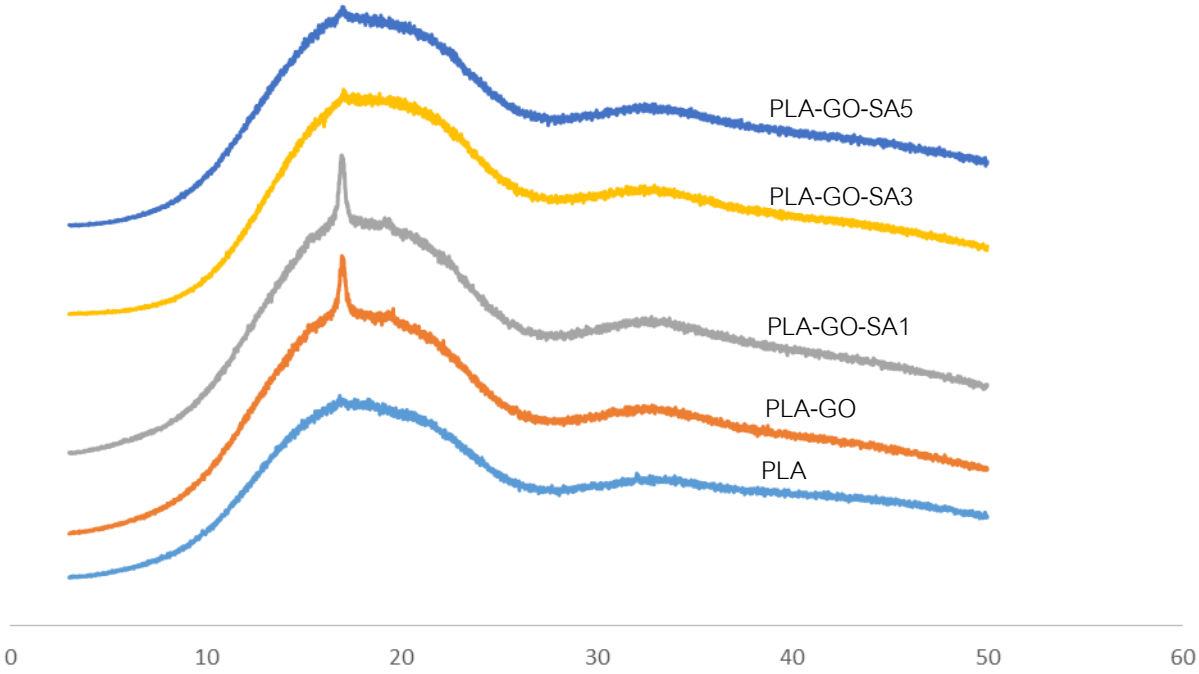

Figure 4. XRD pattern of PLA, PLA-GO, PLA-GO-SA1, PLA-GO-SA3 and PLA-GO-SA5

Fig. 4 shows the XRD patterns of PLA, PLA-GO1-SA1, PLA-GO1-SA3, and PLA-GO1-SA5. The XRD pattern of GO shows a diffraction peak at xx o. The XRD pattern of PLA shows no diffraction peak over the whole range of 2Θ, indicating the amorphous structure of PLA. Addition of GO to PLA can enhance crystallinity in the PLA matrix resulting in one diffraction peak at 17^{o} which is ascribed to the existence of a GO phase in PLA. However, the XRD pattern of PLA-GO1-SA1 shows a similar trend as in the diffraction peak of PLA-GO1, which can be interpreted as that SA addition to GO at 1:1 weight ratio is a suitable ratio that can help stabilize the crystallinity of the GO in the PLA matrix. In contrast, addition of SA to GO at 3:1 and 5:1 weight ratios (PLA-GO1-SA3 and PLA-GO1-SA5) show very small diffraction peaks at the same position as in PLA-GO1 and PLA-GO1-SA1. This could suggest that the content of GO is low and polymer matrix is rich with SA, resulting in a more amorphous structure in the PLA matrix.

Thermal analysis (DSC)

Table 1. Themal properties of PLA, PLA-GO1, PLA-GO1-SA1, PLA-GO1-SA3 and PLA-GO1-SA5 films

	T_g	T_m (°C)	ΔH_m (J/g)	ΔS_m (J/g °C)	T_c (°C)	ΔH_c (J/g)
PLA	59.5	153.3	11.4	0.075	123.3	10.3
PLA-GO1	60.9	153.2	3.4	0.022	131.3	2.1
PLA-GO1-SA 1	58.1	151.3	27.5	0.182	-	-
PLA-GO1-SA 3	57.4	150	26.9	0.179	-	-
PLA-GO1-SA 5	57.2	150	26.2	0.174	-	-

Thermal analysis of PLA, PLA-GO1, PLA-GO1-SA1, PLA-GO1-SA3 and PLA-GO1-SA5 films are shown in Table 1. It can be observed that addition of graphene to PLA does not affect T_g and T_m while addition of stearic acid to PLA-GO1 can decrease T_g and T_m because of amorphization. ΔH_m values of PLA-GO1-SA1, PLA-GO1-SA3 and PLA-GO1-SA5 films are significantly increased more than 2 times and 8 times comparing to PLA and PLA-GO1 respectively. We can determine ΔS_m by the following equation [22];

$$T_m = \frac{\Delta H_m}{\Delta S_m}$$

It can be seen that the increases of ΔH_m and ΔS_m are in proportion. Stearic acid addition to PLA can increase the chain entanglement leading to entropy increment. However, ΔH_c of PLA-GO1 decreases almost 5 times comparing to PLA because graphene itself may hinder the crystallization and molecular rearrangement in PLA matrix. Furthermore, there are no T_c and ΔH_c observed in PLA-GO-SA1, PLA-GO-SA3 and PLA-GO-SA5 samples. This can be explained from two aspects. Firstly, the molecular orientation was suppressed by graphene addition. Secondly, stearic acid added to GO can form chain or brush structure on GO surface resulting in the disorder of molecular orientation or entangled polymer chain.

Mechanical properties

Table 2. Tensile properties of PLA, PLA-GO 1 %wt, PLA-GO 2 %wt, PLA-GO 3 %wt, PLA-GO1-SA1, PLA-GO1-SA3 and PLA-GO1-SA5 films

	Tensile strength (MPa)	Elongation at break (%)	Modulus (Gpa)
PLA	37.0 ± 2.6	48.0 ± 18.9	0.255 ± 0.026
PLA-GO 1 %wt	38.8 ± 2.1	2.5 ± 0.4	0.260 ± 0.028
PLA-GO 2 %wt	38.3 ± 1.8	3.1 ± 0.4	0.232 ± 0.040
PLA-GO 3 %wt	38.8 ± 0.9	3.6 ± 0.2	0.033 ± 0.008
PLA-GO-SA1	49.4 ± 0.3	2.5 ± 0.3	0.289 ± 0.003
PLA-GO-SA3	45.7 ± 2.3	2.6 ± 0.3	0.325 ± 0.018
PLA-GO-SA5	44.4 ± 1.9	2.7 ± 0.4	0.325 ± 0.019

To study the effect of the incorporation of GO and stearic acid to PLA on the mechanical properties of the composites. Tensile modulus, Elongation at break and Modulus of PLA, PLA with GO 1, 2 and 3 weight percent, PLA-GO-SA1, PLA-GO-SA3 and PLA-GO-SA5 samples were measured and listed in Table 2. The tensile strength of neat PLA shows a tensile strength of 37.0 ± 2.6 Mpa with elongation at break of 48.0 ± 18.9 % while the tensile strength of GO addition of 1, 2 and 3 percent to PLA is approximately around 39 Mpa. This value is approximately the same as in PLA. It can be seen that addition of GO to PLA does not improve the mechanical properties of PLA even at high concentration of 3 weight percent. However, when stearic acid was added to PLA-GO1. It can be observed that tensile strength is much improved to 49.4 ± 0.3, 45.7 ± 2.3 and 44.4 ± 1.9 Mpa for PLA-GO-SA1, PLA-GO-SA3 and PLA-GO-SA5 respectively, which can be attributed to the improvement of the dispersion of GO in PLA matrices. These tensile strengths are higher than previously published work on poly(lactic acid)/epoxidized Palm Oil/graphene nanoplatelets composites [23]. PLA-GO-SA1 shows superior tensile strength, more than 33 percent comparing to neat PLA. The compatibility of GO to PLA resulted from the long hydrophobic alky chain from stearic acid. Nevertheless, the elongation at break is still low because necking is not observed in the PLA composites samples.

SEM morphology

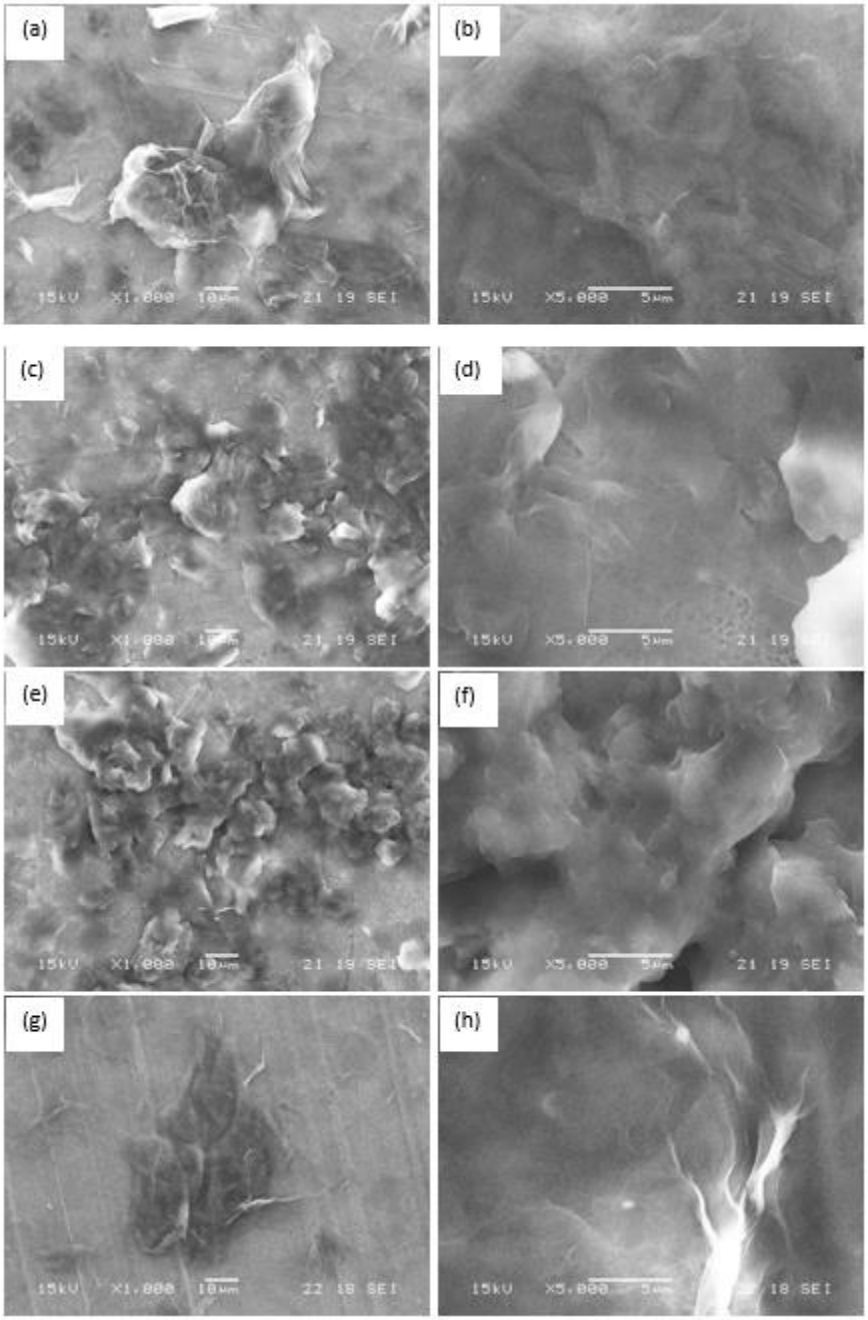

Figure 5. SEM images of GO-SA1 : (a) 1000x mag, (b) 5000x mag; GO-SA3 : (c) 1000x mag, (d) 5000x mag; GO-SA5 : (e) 1000x mag, (f) 5000x mag; and GO : (g) 1000x mag, (h) 5000x mag;

The morphology of GO, GO-SA1, GO-SA3 and GO-SA5 at 1000x and 5000x are shown in Fig. 5a to h. It can be seen that addition of stearic acid to GO at 1 weight ratio resulted in a coating structure of GO by SA film (Fig. 5a and b). At high magnification 5000x, wrinkle is still observed on GO-SA1 comparing to neat GO (Fig. 5g and h). However, adding stearic acid to GO at high concentration of 3 and 5 weight percent, the morphology of GO-SA3 and GO-SA5 becomes agglomerated and tend to lump (Fig. 5c and f). Furthermore, when SA was added to GO, it appears that GO was encapsulated by stearic acid and GO might be restacked at this stage resulting in a raman shift as shown in Fig 1b.

The SEM observations of specimen cross-sections of PLA, PLA-GO, PLA-GO-SA1, PLA-GO-SA3 and PLA-GO-SA5 at 1000x are shown in Fig. 6a to e. It can be observed that the polymer matrices of PLA and PLA-GO samples (Fig. 6a and b) are not smooth. There are many pores observed in the cross-section specimens, indicating non-homogeneous dispersion of GO in the polymer matrix. SEM cross-section images of PLA-GO-SA1, PLA-GO-SA3 and PLA-GO-SA5 (Fig. 6c and e) show smoother and more homogeneous polymer matrices proportional to the amount of SA addition. This can be an indication that the compatibility of GO to PLA can be enhanced by using stearic acid. Nevertheless, high amounts of stearic acid added to GO resulted in stearic acid predominant phases which can lower tensile strength, as discussed in a previous section.

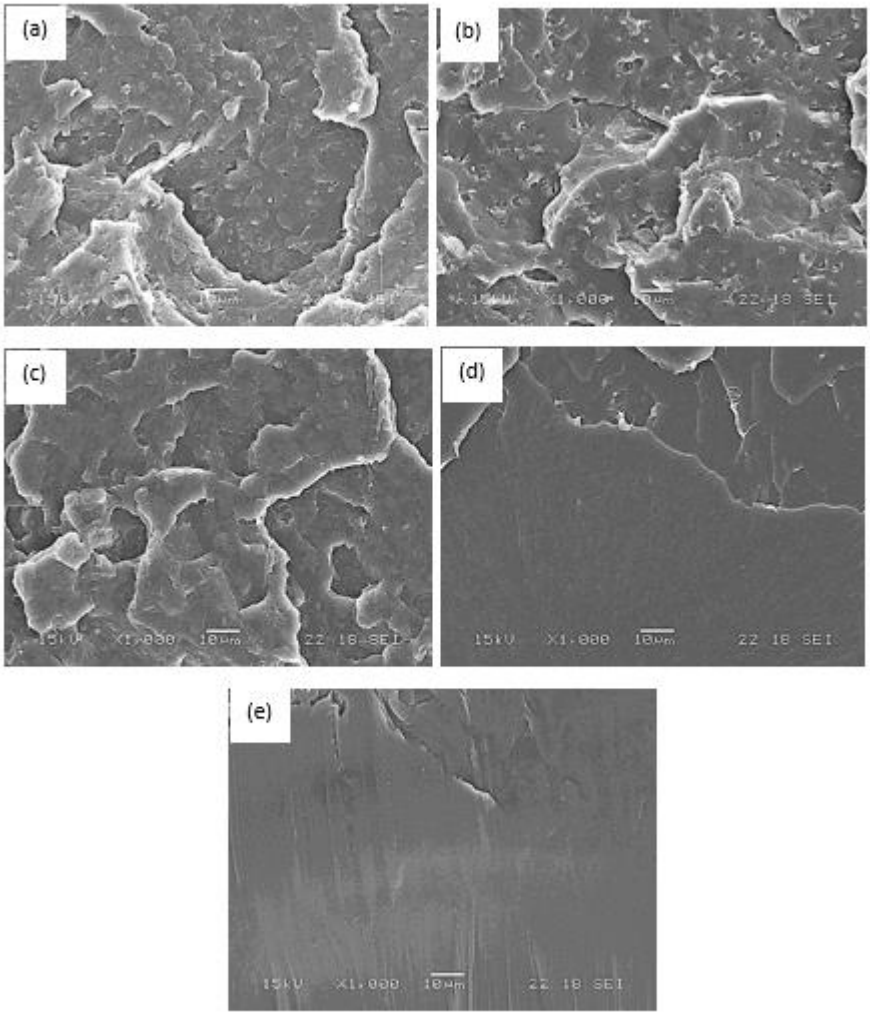

Figure 6. SEM images of polymer composite films at 1000x mag of (a) PLA, (b) PLA-GO, (c) PLA-GO-SA1, (d) PLA-GO-SA3, (e) PLA-GO-SA5

Trans-esterification

In the last section, we used titanium butoxide to catalyze the trans-esterification process during the fabrication of PLA-GO-SA1 film. Schematic illustration of the mechanism of trans-esterification of PLA-GO-SA1-TiBuO4 has been proposed in Fig.7 The film sample was designated as PLA-GO-SA1-TiBuO4. Thermal analysis shows T_g, T_m and T_c at 59.8, 154.2 and 121.5 ^oC respectively. ΔH_m and ΔH_C were found to be 11.3 and 9.8 J/g and ΔS_m is equal to 0.073 J/g ^oC. As we discussed previously, all PLA-GO-SA samples show no T_c and ΔH_C while these values are available for PLA-GO-SA1-TiBuO4. This can be confirmation that there was a molecular orientation in PLA-GO-SA1-TiBuO4 that was beneficial to tensile strength. Tensile strength of PLA-GO-SA1-TiBuO4 was 51.9 ± 3.7 Mpa which is higher than PLA-GO-SA1, while elongation at break and modulus are nearly the same and were found to be 3.2 ± 0.3 % and 0.275 ± 0.019 GPa respectively.

The XRD pattern of PLA-GO-SA1-TiBuO4 film (Fig. 8) shows a sharp diffraction peak at the same position as observed in PLA-GO-SA1 (17 ^{o}). Thermal analysis and diffraction pattern data confirm that the polymer structure of PLA-GO-SA1-TiBuO4 film is more crystalline showing a different case comparing to PLA-SA1, PLA-SA3, PLA-SA5 films.

The SEM observations of a specimen cross-section of PLA-GO1-SA1-TiBuO4 film (Fig. 9a to c) illustrate a lot of whiskers throughout the cracking surface, which is different from PLA-GO-SA1, PLA-GO-SA3, PLA-GO-SA5. It can be implied that sample cracking in PLA-GO-SA1-TiBuO4 may be different from the others and also the whiskers are the influence of the tensile strength increment.

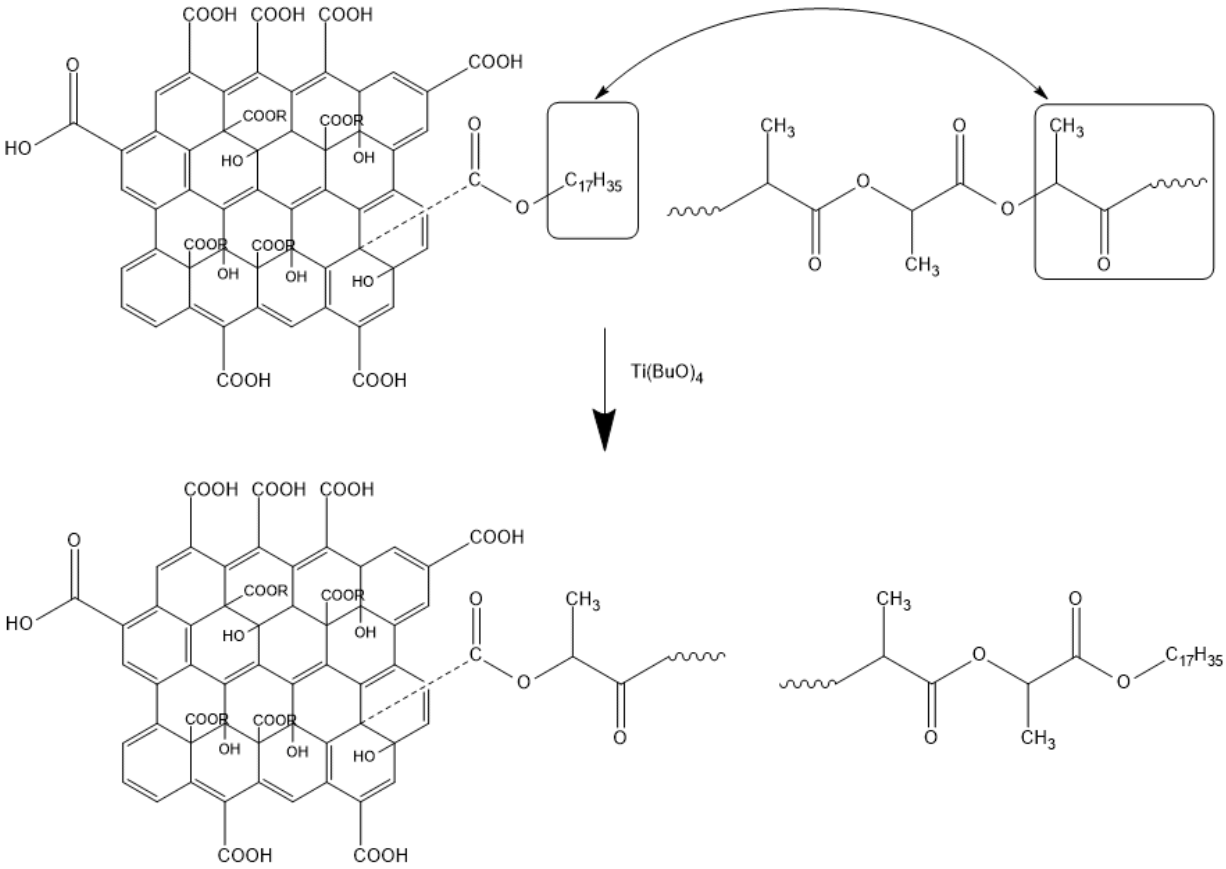

Figure 7. Schematic illustration of the mechanism of trans-esterification of PLA-GO-SA1-TiBuO4

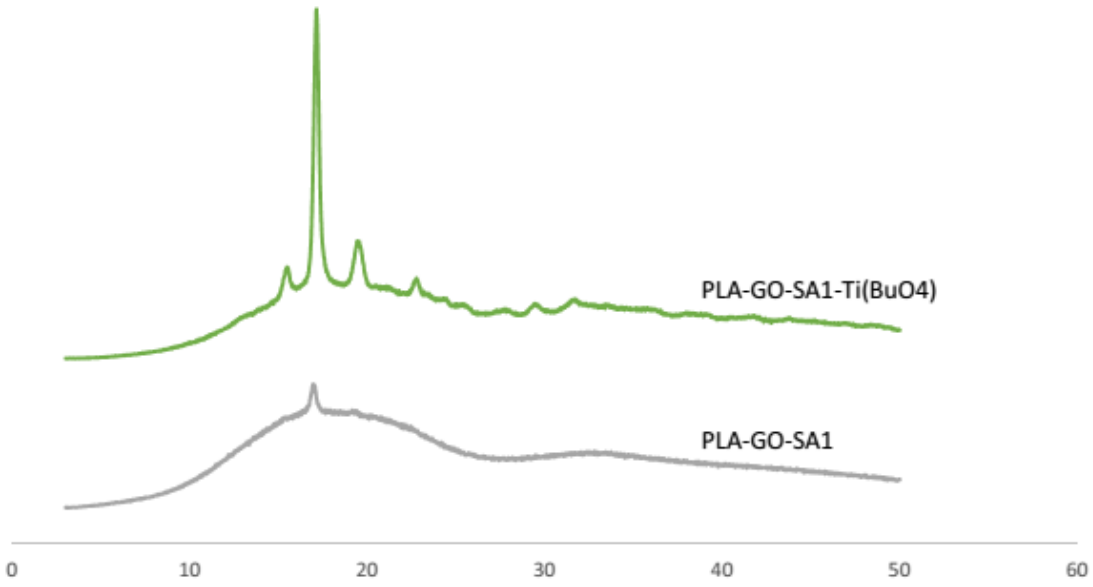

Figure 8. XRD pattern of PLA-GO-SA1 compared to PLA-GO-SA1-Ti(BuO4)

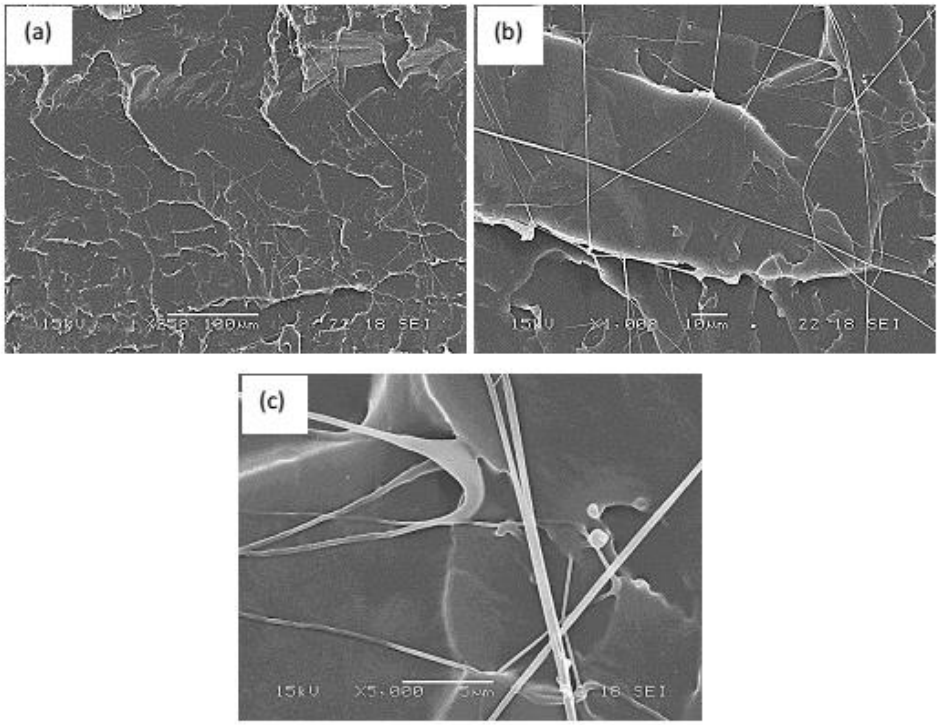

Figure 9. SEM images of polymer composite films of PLA-GO1-SA1-TiBuO4 : (a) 250x mag, (b) 1000x mag and (c) 5000x mag

Conclusion

Graphene /Poly (lactic acid)/Stearic acid composites have been successfully fabricated. The obtained results show that stearic acid attached on GO sheets can act as a compatibilizer of GO to PLA matrices. The outcome is that tensile strength is improved, especially in PLA-GO1-SA1 and PLA-GO1-SA1-TiBuO4 where the observed tensile strengths are more than 33 and 40 percent higher respectively, comparing to neat PLA. The compatibility of GO to PLA influenced by stearic acid results from the lipophilicity increment of the long hydrophobic alky chain. However, stiffness can be observed in all PLA-GO-SA samples due to the absence of necking in the PLA composites samples.

Acknowledgement

The authors would like to thank the Thailand Research Fund, Office of the Higher Education Commission and University of Phayao for their financial support.

References

1. Flieger, M., et al., *Biodegradable plastics from renewable sources.* Folia Microbiologica, 2003. **48**(1): p. 27-44.
2. Pathak, S., C. Sneha, and B.B. Mathew, *Bioplastics: Its Timeline Based Scenario & Challenges.* Journal of Polymer and Biopolymer Physics Chemistry, 2014. **2**(4): p. 84-90.
3. Song, J.H., et al., *Biodegradable and compostable alternatives to conventional plastics.* Philosophical Transactions of the Royal Society B: Biological Sciences, 2009. **364**(1526): p. 2127-2139.
4. Lee, C., et al., *Measurement of the Elastic Properties and Intrinsic Strength of Monolayer Graphene.* Science, 2008. **321**(5887): p. 385-388.
5. Bolotin, K.I., et al., *Ultrahigh electron mobility in suspended graphene.* Solid State Communications, 2008. **146**(9–10): p. 351-355.
6. Balandin, A.A., et al., *Superior Thermal Conductivity of Single-Layer Graphene.* Nano Letters, 2008. **8**(3): p. 902-907.
7. Stankovich, S., et al., *Graphene-based composite materials.* Nature, 2006. **442**(7100): p. 282-286.
8. Ou, B., et al., *Covalent functionalization of graphene with poly(methyl methacrylate) by atom transfer radical polymerization at room temperature.* Polymer Chemistry, 2012. **3**(10): p. 2768-2775.
9. Pham, V.H., et al., *Highly Conductive Poly(methyl methacrylate) (PMMA)-Reduced Graphene Oxide Composite Prepared by Self-Assembly of PMMA Latex and Graphene Oxide through Electrostatic Interaction.* ACS Applied Materials & Interfaces, 2012. **4**(5): p. 2630-2636.

10. Wu, S.-D., et al., *A graphene/poly(vinyl alcohol) hybrid membrane self-assembled at the liquid/air interface: enhanced mechanical performance and promising saturable absorber.* Journal of Materials Chemistry, 2012. **22**(33): p. 17204-17209.
11. Wang, J., et al., *Preparation of graphene/poly(vinyl alcohol) nanocomposites with enhanced mechanical properties and water resistance.* Polymer International, 2011. **60**(5): p. 816-822.
12. Qi, X.-Y., et al., *Enhanced Electrical Conductivity in Polystyrene Nanocomposites at Ultra-Low Graphene Content.* ACS Applied Materials & Interfaces, 2011. **3**(8): p. 3130-3133.
13. Du, J. and H.-M. Cheng, *The Fabrication, Properties, and Uses of Graphene/Polymer Composites.* Macromolecular Chemistry and Physics, 2012. **213**(10-11): p. 1060-1077.
14. Ferrari, A.C., *Raman spectroscopy of graphene and graphite: Disorder, electron–phonon coupling, doping and nonadiabatic effects.* Solid State Communications, 2007. **143**(1–2): p. 47-57.
15. Zhu, Y., et al., *Graphene and Graphene Oxide: Synthesis, Properties, and Applications.* Advanced Materials, 2010. **22**(35): p. 3906-3924.
16. Chartarrayawadee, W., et al., *Facile synthesis of reduced graphene oxide/MWNTs nanocomposite supercapacitor materials tested as electrophoretically deposited films on glassy carbon electrodes.* Journal of Applied Electrochemistry, 2013. **43**(9): p. 865-877.
17. Wang, Y.y., et al., *Raman Studies of Monolayer Graphene: The Substrate Effect.* The Journal of Physical Chemistry C, 2008. **112**(29): p. 10637-10640.
18. Shin, H.-J., et al., *Efficient Reduction of Graphite Oxide by Sodium Borohydride and Its Effect on Electrical Conductance.* Advanced Functional Materials, 2009. **19**(12): p. 1987-1992.
19. Das, A., B. Chakraborty, and A.K. Sood, *Raman spectroscopy of graphene on different substrates and influence of defects.* Bulletin of Materials Science, 2008. **31**(3): p. 579-584.
20. Yang, H., et al., *Rapid and non-destructive identification of graphene oxide thickness using white light contrast spectroscopy.* Carbon, 2013. **52**(0): p. 528-534.

21. Stankovich, S., et al., *Synthesis of graphene-based nanosheets via chemical reduction of exfoliated graphite oxide.* Carbon, 2007. **45**(7): p. 1558-1565.
22. Ramakrishnan, M., et al., *Differential scanning calorimetric studies on the thermotropic phase transitions of dry and hydrated forms of N-acylethanolamines of even chainlengths.* Biochimica et Biophysica Acta (BBA) - Biomembranes, 1997. **1329**(2): p. 302-310.
23. Chieng, B.W., et al., *Graphene Nanoplatelets as Novel Reinforcement Filler in Poly(lactic acid)/Epoxidized Palm Oil Green Nanocomposites: Mechanical Properties.* International Journal of Molecular Sciences, 2012. **13**(9): p. 10920-10934.

Future work

Metallic nanoparticles will be incorporate to PLA-GO-SA natrix to investigate their properties enhancement. For example, mechanical properties, thermal properties and conducting properties.

Output จากโครงการวิจัยที่ได้รับทุนจาก สกว.

1. ผลงานตีพิมพ์ในวารสารวิชาการนานาชาติ
   อยู่ในระหว่างการยื่น manuscript เพื่อตีพิมพ์ในวารสารวิชาการนานาชาติ
2. การนำผลงานวิจัยไปใช้ประโยชน์
   - ได้มีการนำไปบูรณาการกับการเรียนการสอนในรายวิชาเคมีเชิงฟิสิกส์ ปัญหาพิเศษทางเคมีและการค้นคว้าอิสระ
3. อื่นๆ (เช่น ผลงานตีพิมพ์ในวารสารวิชาการในประเทศ การเสนอผลงานในที่ประชุมวิชาการ หนังสือ การจดสิทธิบัตร)